Homology Modeling and Docking studies of a Δ9-fatty acid desaturase from a Cold-tolerant Pseudomonas sp. AMS8

Lawal Garba [1, 2, 3], **Mohamad Ariff Mohamad Yussoff** [4], **Khairul Bariyyah Abd Halim** [4], **Siti Nor Hasmah Ishak** [1], **Mohd Shukuri Mohamad Ali** [1, 5], **Siti Nurbaya Oslan** [1, 5], **Raja Noor Zaliha Raja Abd. Rahman** Corresp. [1, 2]

[1] Enzyme and Microbial Technology Research Centre, Faculty of Biotechnology and Biomolecular Sciences, Universiti Putra Malaysia, Serdang, Selangor, Malaysia
[2] Department of Microbiology, Faculty of Biotechnology and Biomolecular Sciences, Universiti Putra Malaysia, Serdang, Selangor, Malaysia
[3] Department of Microbiology, Faculty of Science, Gombe State University, Gombe, Gombe state, Nigeria
[4] Department of Biotechnology, Kulliyyah of Science, International Islamic University, Kuantan, Pahang Darul Makmur, Malaysia
[5] Department of Biochemistry, Faculty of Biotechnology and Biomolecular Sciences, Universiti Putra Malaysia, Serdang, Selangor, Malaysia

Corresponding Author: Raja Noor Zaliha Raja Abd. Rahman
Email address: rnzaliha@upm.edu.my

Membrane-bound fatty acid desaturases perform oxygenated desaturation reactions to insert double bonds within fatty acyl chains in regioselective and stereoselective manners. The Δ9-fatty acid desaturase strictly creates the first double bond between C9 and 10 positions of most saturated substrates. As the three-dimensional structures of the bacterial membrane fatty acid desaturases are not available, relevant information about the enzymes are derived from their amino acid sequences, site-directed mutagenesis and domain swapping in similar membrane-bound desaturases. The Cold-tolerant Pseudomonas sp. AMS8 was found to produce high amount of monounsaturated fatty acids at low temperature. Subsequently, an active Δ9-fatty acid desaturase was isolated and functionally expressed in Escherichia coli. In this paper we report homology modeling and docking studies of a Δ9-fatty acid desaturase from a Cold-tolerant Pseudomonas sp. AMS8 for the first time to the best of our knowledge. Three dimensional structure of the enzyme was built using MODELLER version 9.18 using a suitable template. The protein model contained the three conserved-histidine residues typical for all membrane-bound desaturase catalytic activity. The structure was subjected to energy minimization and checked for correctness using Ramachandran plot and ERRAT, which showed a good quality model of 91.6 and 65.0%, respectively. The protein model was used to preform MD simulation and docking of palmitic acid using CHARMM36 force field in GROMACS Version 5 and Autodock tool Version 4.2, respectively. The docking simulation with the lowest binding energy, -6.8 kcal/mol had a number of residues in close contact with the docked palmitic acid namely, Ile26, Tyr95, Val179, Gly180, Pro64, Glu203, His34, His206, His71, Arg182, Thr85, Lys98 and His177. Interestingly, among the binding residues are His34, His71 and His206 from the first, second, and third conserved histidine motif, respectively

which constitute the active site of the enzyme. The results obtained are in compliance with the in vivo activity of the Δ9-fatty acid desaturase on the membrane phospholipids.

Homology Modeling and Docking studies of a Δ9-fatty acid desaturase from a Cold-tolerant *Pseudomonas* sp. AMS8

Lawal Garba[1, 2,3], Mohamad Ariff Mohamad Yussoff[4], Khairul Bariyyah Abd Halim[4], Siti Nor Hasmah Ishak[1], Mohd Shukuri Mohamad Ali[1,5], Siti Nurbaya Oslan[1,5] and Raja Noor Zaliha Raja Abdul Rahman*[1,2]

1. Enzyme and Microbial Technology Research Centre, Faculty of Biotechnology and Biomolecular Sciences, University Putra Malaysia, Serdang, Selangor, Malaysia.
2. Department of Microbiology, Faculty of Biotechnology and Biomolecular Sciences, University Putra Malaysia, Serdang, Selangor, Malaysia.
3. Department of Microbiology, Faculty of Science, Gombe State University, Gombe, Gombe State, Nigeria.
4. Department of Biotechnology, Kulliyyah of Science, International Islamic University Malaysia, Kuantan, Pahang Darul Makmur, Malaysia.
5. Department of Biochemistry, Faculty of Biotechnology and Biomolecular Sciences, University Putra Malaysia, Serdang, Selangor, Malaysia.

*Corresponding author:

Raja Noor Zaliha Raja Abd. Rahman,

Enzyme and Microbial Technology Research Centre, Faculty of Biotechnology and Biomolecular Sciences, University Putra Malaysia, 43400 UPM Serdang, Selangor Darul Ehsan, Malaysia

Phone number: +60192760708

Email: rnzaliha@upm.edu.my

Abstract

Membrane-bound fatty acid desaturases perform oxygenated desaturation reactions to insert double bonds within fatty acyl chains in regioselective and stereoselective manners. The Δ9-fatty acid desaturase strictly creates the first double bond between C9 and 10 positions of most saturated substrates. As the three-dimensional structures of the bacterial membrane fatty acid desaturases are not available, relevant information about the enzymes are derived from their amino acid sequences, site-directed mutagenesis and domain swapping in similar membrane-bound desaturases. The Cold-tolerant *Pseudomonas* sp. AMS8 was found to produce high amount of monounsaturated fatty acids at low temperature. Subsequently, an active Δ9-fatty acid desaturase was isolated and functionally expressed in *Escherichia coli*. In this paper we report homology modeling and docking studies of a Δ9-fatty acid desaturase from a Cold-tolerant *Pseudomonas* sp. AMS8 for the first time to the best of our knowledge. Three dimensional structure of the enzyme was built using MODELLER version 9.18 using a suitable template. The protein model contained the three conserved-histidine residues typical for all membrane-bound desaturase catalytic activity. The structure was subjected to energy minimization and checked for correctness using Ramachandran plot and ERRAT, which showed a good quality model of 91.6 and 65.0%, respectively. The protein model was used to preform MD simulation and docking of palmitic acid using CHARMM36 force field in GROMACS Version 5 and Autodock tool Version 4.2, respectively. The docking simulation with the lowest binding energy, -6.8 kcal/mol had a number of residues in close contact with the docked palmitic acid namely, Ile26, Tyr95, Val179, Gly180, Pro64, Glu203, His34, His206, His71, Arg182, Thr85, Lys98 and His177. Interestingly, among the binding residues are His34, His71 and His206 from the first, second, and third conserved histidine motif, respectively which constitute the active site of the enzyme. The results obtained are in

compliance with the *in vivo* activity of the Δ9-fatty acid desaturase on the membrane phospholipids.

Introduction

Fatty acid desaturase enzymes perform desaturation reactions which strictly create a double bond within fatty acyl chain in regioselective and stereoselective manners. Phylogenetically, the enzymes have been broadly divided into two unrelated classes as the acyl-acyl carrier protein and membrane-bound fatty acid desaturases. The class of the acyl-acyl carrier proteins specifically catalyses the production of oleic acid (C18:1) from stearic acid (C18:0) in plants whereas that of the membrane-bound desaturases represent the most widely distributed form of the enzymes predominantly found in bacteria and eukaryotes (Hashimoto *et al.*, 2008; Kachroo *et al.*, 2007).

In the mechanism of oxygen-dependent desaturation reactions, the fatty acid desaturases activate molecular oxygen using their active-site diiron centre which is shared by several proteins such as ribonucleotide reductase, methane monooxygenase, rubrerythrins, and a range of oxidase enzymes. Relevant information about the tuning of the diiron centers in relation to various chemical reactivity have been made available through comparisons of the diiron clusters of many diiron-containing enzymes (Sazinsky and Lippard, 2006; Shanklin *et al.*, 2009; Yoon and Lippard, 2004). Nevertheless, disparities in various protein to protein interactions, amino acid sequence and reaction outcomes confound the analysis. Research on fatty acid desaturases and similar enzymes created an avenue to conducting structure-function analyses due to a wide range of reactions performed on like substrates by the close homologous enzymes (Lee *et al.*, 1998; Shanklin and Cahoon, 1998; Shanklin *et al.*, 2009).

The amino acid sequences of both the integral membrane desaturases in (bacteria and eukaryotes) and acyl-acyl carrier protein desaturases of plants contain conserved histidine boxes predicted as the essential catalytic sites of the enzymes (Alonso *et al.*, 2003). However, the former enzymes contained three conserved-histidine motifs labelled as 'HXXXXH', 'HXXHH' and HXXHH' whereas the latter contained twice conserved-histidine motifs as EXXH (Alonso *et al.*, 2003; Lindqvist *et al.*, 1996) . As the three-dimensional structures of the bacterial membrane fatty acid desaturases are still unavailable, relevant information about the enzymes are derived from the amino acid sequences, site-directed mutagenesis, and domain swapping in similar membrane-bound desaturases coupled with homology modelling(Venegas-Calerón *et al.*, 2006). The Cold-tolerant *Pseudomonas* sp. A8 was able to produce high amount of monounsaturated fatty acids at 4 ^{o}C (Lawal *et al.*, 2016). Subsequently, an active Δ9-fatty acid desaturase was isolated and functionally expressed in *Escherichia coli.* The enzyme was found to catalyse conversion from membrane associated palmitic to palmitoleic acid (Garba *et al.*, 2016a). In this paper we report homology modeling and docking studies of Δ9-fatty acid desaturase from a Cold-tolerant *Pseudomonas* sp. A8 with palmitic acid as a substrate for the first time to the best of our knowledge.

Materials and Methods

Templates selection

BLASTP of the target protein was performed at the NCBI (https://blast.ncbi.nlm.nih.gov/Blast.cgi?PROGRAM=blastp) which showed identity of 24 and 23% to human integral membrane stearoyl-CoA desaturase (PDB ID: 4ZYO) and mouse stearoyl-coA desaturase (PDB ID: 4YMK). However, the mouse stearoyl-coA desaturase (PDB ID: 4YMK) was chosen as a template (based on its high resolution) to predict the three dimensional structure of the Δ9-fatty acid desaturase.

Structure prediction

The primary sequences of human (Uniprot ID:O00767) and mouse (Uniprot ID:P13516) desaturases were obtained from Uniprot protein databases. Moreover, the protein sequences of Δ9-fatty acid desaturases from several other *Pseudomonas* species were obtained from the GenBank. The transmembrane (TM) spanning region of *Pseudomonas* sp. A8 Δ9-fatty acid desaturase was predicted using a TM domain topology prediction program, CCTOP (http://cctop.enzim.ttk.mta.hu/). The CCTOP predicted the TM domains of the protein sequence based on the consensus of ten (10) different methods (Dobson *et al.*, 2015a, 2015b). The TM domains were modelled together with the remaining amino acid residues toward the C-terminus of the protein using MODELLER version 9.18 (Webb and Sali, 2014). Alignment input used in the MODELLER was derived from the pairwise alignments of both the template and model primary sequences using membrane proteins alignment tool (Stamm *et al.*, 2013) whereas the secondary structure was predicted using PSIPRED tool (Buchan *et al.*, 2013) and used as a guide to modelling the C-terminal domain.

Energy minimization and Quality verification

The protein model generated by the MODELLER was ranked and scored using discrete optimised protein energy (DOPE) score. The top three models out of 50 models with the lowest DOPE scores were chosen and assessed using ERRAT and RAMPAGE server. The best model was selected for energy minimization to remove clashes between side chains using GROMACS and subsequently used in docking and molecular dynamics simulations. Further structural assessment was performed by simulating the homology models inside a membrane bilayer.

Active site Prediction

Prior to docking simulations, the binding site for the *Pseudomonas* sp. A8 model was predicted using COACH (Buchan *et al.*, 2013). The predicted active site was found in the vicinity of histidine rich region, which served as an already established potential binding site of the enzyme (this site was used for a targeted docking). Blind docking was also performed to bind palmitate on both the template and model structures.

Docking studies

Three dimensional (3D) structure of palmitic acid was obtained from the Pubchem (https://pubchem.ncbi.nlm.nih.gov). The energy minimized model of the Δ9-fatty acid desaturase and the palmitic acid (ligand) were prepared and used for molecular docking of the substrate onto the target proteins using Autodock tool Version 4.2 (Trott and Olson, 2010). Blind docking of the palmitate onto the modelled structure was performed using a pre-set simulation grid box size of 126x126x126 Å along the X,Y and Z axes and centred at 39.946,40.191,45.879 whereas the targeted docking grid box size was set to 70x70x60 Å dimension and centred at 43.946, 40.191,33.879 of X,Y and Z coordinate, respectively. The docking simulations were performed for 100 runs using Lamarckian Genetic Algorithm (LGA). The results were evaluated using RMSD values, ligand-protein interactions, binding energy (ΔG_{bind}) as well as a number of conformations existed in a populated cluster. The ligand-protein interaction was visualized using Pymol (Trott and Olson, 2010) and VMD (Humphrey *et al.*, 1996).

MD simulations

The model structure of the Δ9-fatty acid desaturase was simulated in an embedded 1-palmitoyl-2-oleoyl-sn-glycero-3-phosphocholine (POPC) bilayer. The protein-bilayer system was constructed using CHARMM-GUI Membrane builder (Jo *et al.*, 2008). The atomistic

MD simulations were performed using CHARMM36 force field (Huang and MacKerell, 2013) in GROMACS Version 5 (Pronk *et al.*, 2013) within an integration time step of 20 fs. The simulation temperature was kept constant at 310 K by coupling the system to a heat bath using a Nose-Hoover thermostat with τ_T = 1 ps. Pressure was maintained at 1 atm using a Parinello-Rahman barostat and semiisotropic pressure with τ_P = 5 ps and a compressibility of $4.5e^{-5}$ bar $^{-1}$. Long-range electrostatics were treated using particle mesh Ewald method with a cutoff of 12 Å. The 12 Å cutoff distance was used for van der Waals interactions. The systems were equilibrated for 1 ns restraining the Cα atoms, followed by production runs of 50 ns each in triplicates. The data was analysed using GROMACS tools and VMD.

Results

Sequence of the Δ9-fatty acid desaturase protein and templates identification

The Δ9-fatty acid desaturase was isolated from a Cold-tolerant *Pseudomonas* sp. A8 and functionally expressed in *Escherichia coli* as confirmed by GCMS analysis which showed an active enzyme capable of increasing the overall palmitoleic acid content of the recombinant *E. coli*. Based on the GCMS analysis, a profound increase in the amount of palmitoleic acid from 10.5 to 21% was observed at 20 ^{o}C (Garba *et al.*, 2016a). The protein had a molecular weight of 45 kDa and 394 amino acids which was already deposited at NCBI (accession number: AMX81567). Multiple sequences alignments of the template, the Cold-tolerant *Pseudomonas* sp. A8 Δ9-fatty acid desaturase and sequences from several other Δ9-fatty acid desaturases has revealed the three conserved-histidine boxes common to all membrane-bound desaturases in bacteria (Garba *et al.*, 2016b; Li *et al.*, 2009), fungi (Chen *et al.*, 2013) and animals (Bai *et al.*, 2015) (Figure 1). The human integral membrane stearoyl-CoA desaturase (PDB ID: 4ZYO) and mouse stearoyl-coA desaturase (PDB ID: 4YMK) have been solved to a resolution of 3.25 Å and 2.6 Å, respectively. The two structures share moderate sequence

identities of 24 and 23% with the *Pseudomonas* sp. A8, respectively. However, the mouse stearoyl-coA desaturase was chosen as the template based on its higher resolution.

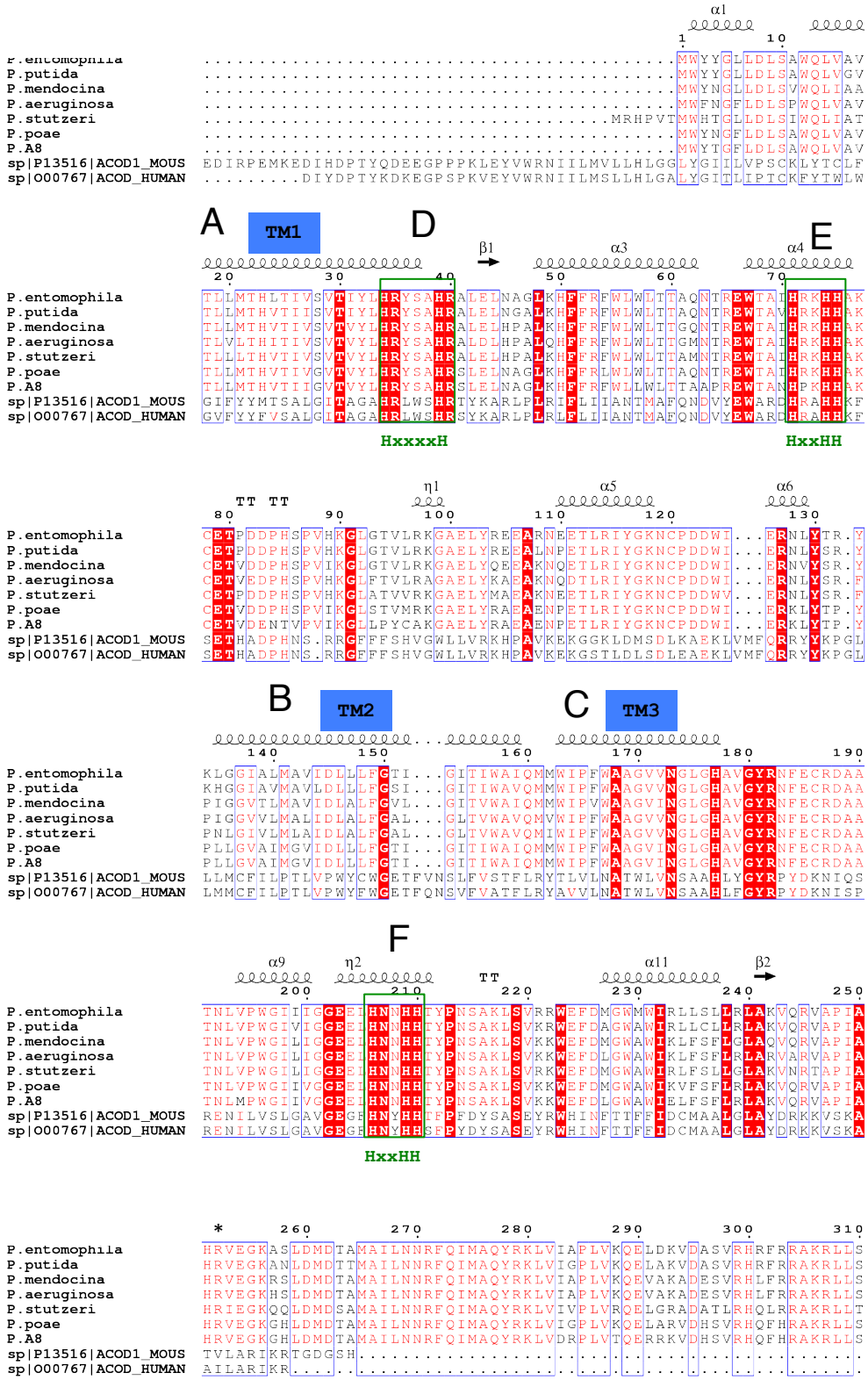

Figure 1: Multiple sequences alignments of protein sequence from *Pseudomonas* sp. A8 Δ9-fatty acid (AMX81567) and sequences from other desaturase proteins. The transmembrane

domains of the protein are indicated by letters A, B and C whereas the three conserved-histidine boxes common to all membrane-bound desaturases are shown by D, E, and F. The end of the model structure is at Arg251 indicated by an asterisk (*).

Model of the Δ9-fatty acid desaturase

To correctly model the TM domain of a membrane protein, it is necessary to appropriately predict its TM spanning region. CCTOP used 11 TM prediction programs including some of the best TM domain predictor such as TMHMM and HMMTOP to predict the TM domain of the target protein. Most of the prediction programs predicted that the target protein has three TM spanning regions as detailed in Figure 2A, which gave a consensus domains of TM1 (Leu13--Leu33), TM2 (Leu135--Ile159) and TM3 (Met162--Tyr181) of 20, 25 and 20 amino acid residues, respectively. However, the TM2 and TM3 were not aligned at the TM domains of the template. Thus, some manual adjustment of the TM2 and TM3 was performed to prepare the alignment input for the MODELLER. As the three dimensional (3D) structure of the template had four TM domains, only three TM3 domains were considered for modelling the P*seudomonas* sp. A8 Δ9-fatty acid desaturase (predicted to have only three TM domains) using MODELLER (Figure 2B). The structure with the lowest DOPE score was assessed and improved after energy minimization and subsequently used for further analyses.

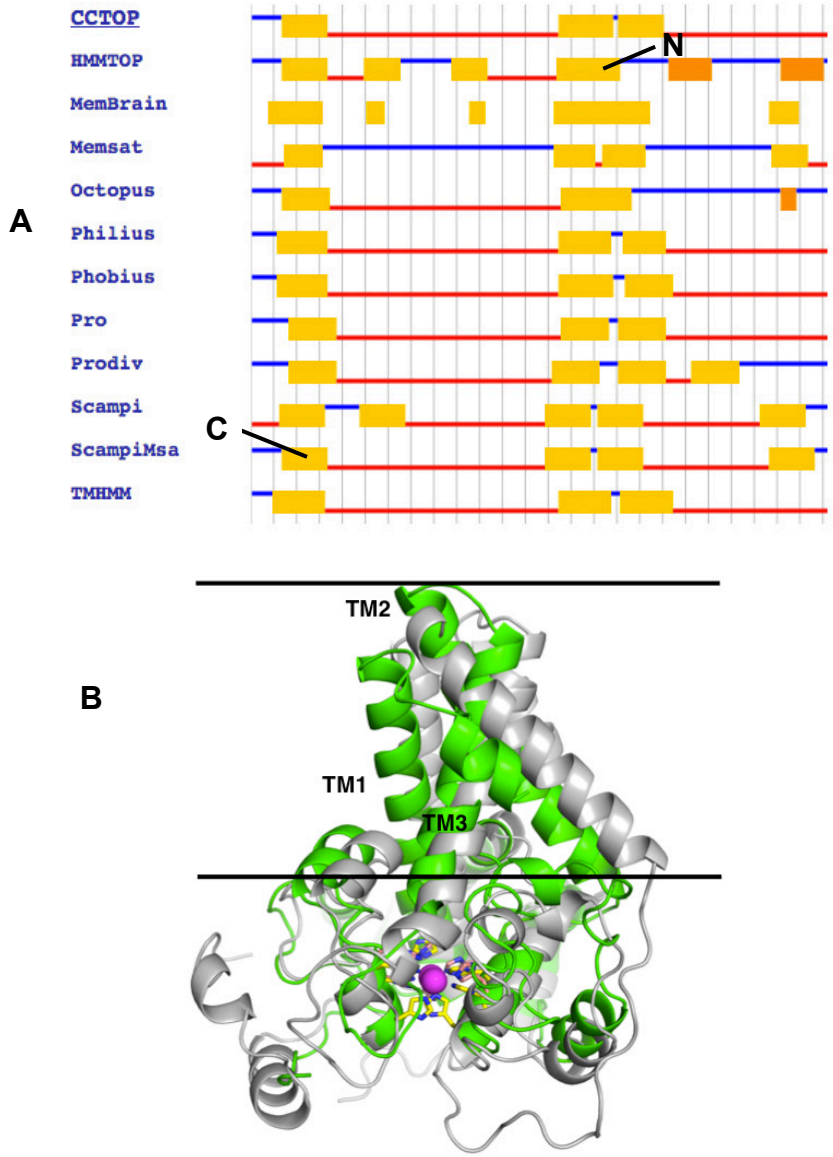

Figure 2: The TM topology as derived from CCTOP prediction A). Superimposed three dimensional model structures of *Pseudomonas* sp. A8 Δ9-fatty acid desaturase (green) and the template from the crystal structure of mouse stearoyl-coenzyme A desaturase (4YMK) shown in grey (B). The Zn ions found in the crystal structure of the mouse desaturase are shown as purple spheres. The approximate position of the bilayer is indicated by the two black lines.

Quality verification of the predicted structure

Quality of protein models are verified using various programmes such as ERRAT and Ramachandran plot which are freely available online servers (Mahgoub and Bolad, 2013). In

this study, the predicted structure that has gone through energy minimization was verified for correctness using the ERRAT and Ramachandran plot. Two models were predicted and labelled as AMX8-em1 and AMX8-em2 (shown in the supplementary files). The ERRAT programme showed an overall quality value of 65.021% for AMX8-em2 (Figure 3). However, AMX8-em2 model was found to be more stable during the simulation experiment therefore, was chosen for further analysis. In general, high resolution structures generate quality values that fall around 95% or higher whereas lower resolution structures produced an average quality factor that is around 91% and the error function is statistically determined on the basis of non-bound atom to atom interactions in the target structure (Colovos and Yeates, 1993). RAMPAGE programme is used to check the overall sterio-chemical quality, local and residue-by-residue reliability usually shown on a Ramachandran plot. The programme shows the sterio-chemistry of the main-chain torsion angles Phi, Psi (φ, ψ) of a good protein model. The Ramachandran plot displays the polypeptide chain of a protein structure using the φ, ψ angles pair (Laskowski *et al.*, 1993; Mahgoub and Bolad, 2013; Ramachandran *et al.*, 1963). Figure 4 and Table 1 indicate that up to 91.6% of the residues fall within the most favoured regions, 6.8% in the allowed regions whereas only 1.6% residues are in the outlier regions, further confirming that the predicted model is of good quality.

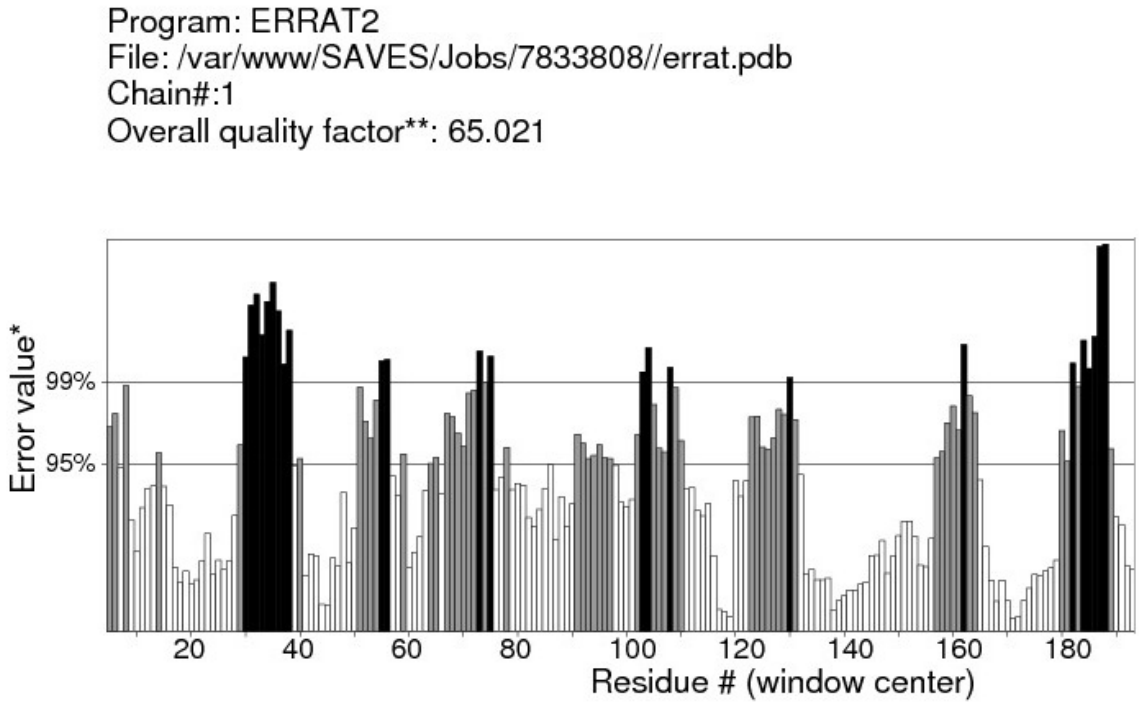

253

254 Figure 3: Quality verification plot of the energy minimized model of the Δ9-fatty acid
255 desaturase performed using ERRAT. The two lines drawn on the error axis show the
256 confidence with which it is possible to reject regions that exceed that error value. Good high
257 resolution structures generally produce values around 95% or higher whereas lower resolution
258 (2.5- -3Å) have an average overall quality factor around 91%.

259

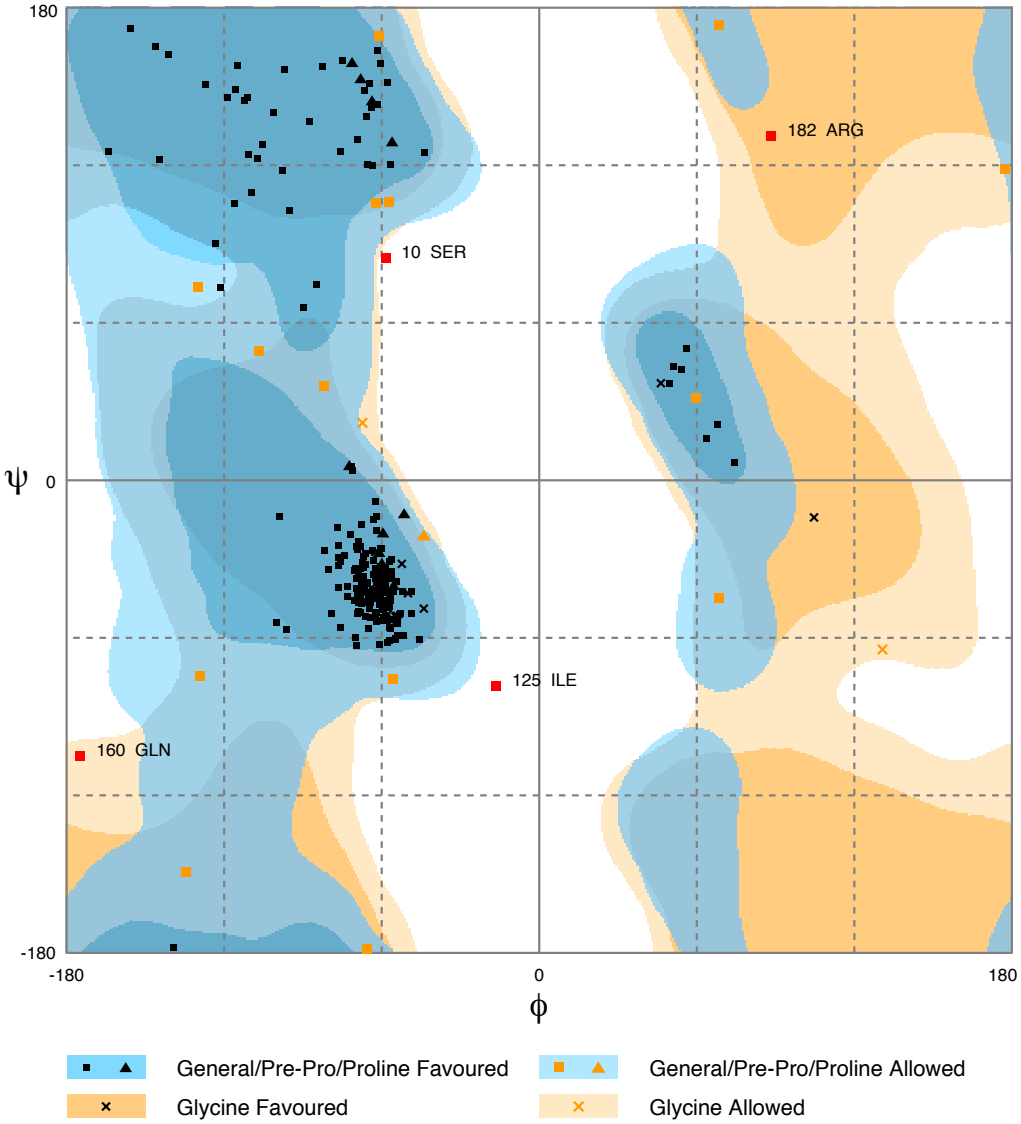

Figure 4: Ramachandran plot of *Pseudomonas* sp. A8 Δ9-fatty acid desaturase model generated by RAMPAGE server.

Table 1: Details of Ramachandran plot after energy minimization

Plot statistics	% after energy minimization
Residues in the most favoured regions	91.6
Residues in allowed regions	6.8
Residues in the outlier region	1.6

Catalytic site of the predicted structure

Membrane-bound desaturases share an exceptional structural resemblance and a wide range of functionality. Three conserved-histidine boxes that are common to all classes of these enzymes function in binding two irons at the catalytic centre. The structural similarity has given an insight into their structure-function relationships (Meesapyodsuk *et al.*, 2007). The predicted structure of *Pseudomonas* sp. A8 Δ9-fatty acid desaturase contains the three conserved-histidine boxes consisting of eight histidine residues at positions 1 (His34, His39), 2 (His71, His74, His75) and 3(His206, His209, His210) from N to C-terminus of the enzyme shown in Figure 5A and analysed in Figure 5B. The conserved-histidine motifs are consistent with those observed during the multiple sequences alignments of the target sequence with the template corresponding to the already established catalytic centre of membrane-bound desaturases. The role of the eight histidine residues in the conserved histidine-rich motifs has been demonstrated through site-directed mutagenesis of rat stearoyl-CoA Δ^9-desaturase whereas those residues flanking the conserved region have critical catalytic properties in plant FAD2 desaturases and related enzymes (Broadwater *et al.*, 2002; Meesapyodsuk *et al.*, 2007; Shanklin *et al.*, 1994).

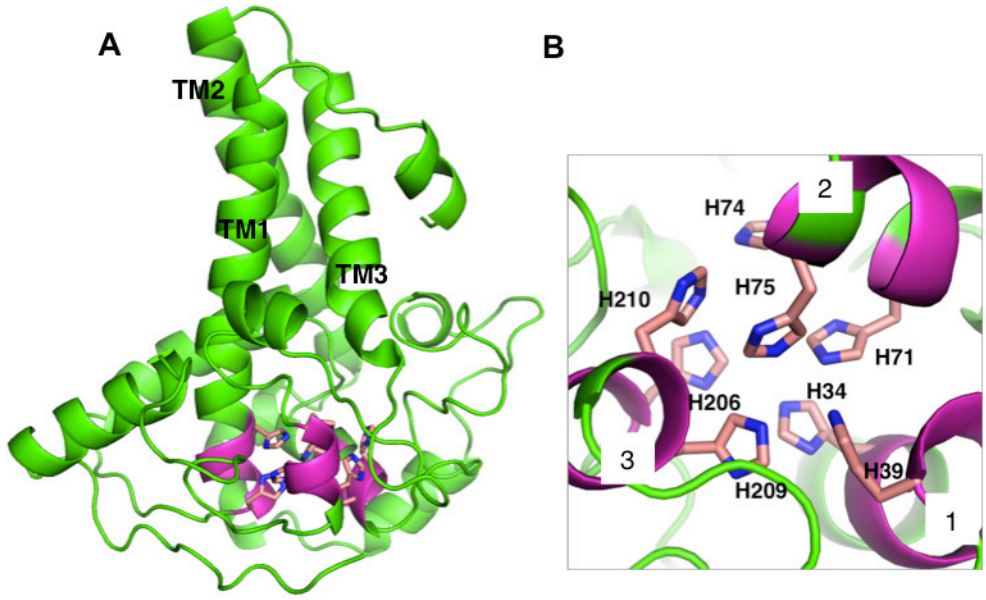

Figure 5: Analysis of *Pseudomonas* sp. A8 Δ9-fatty acid desaturase model showing the overall cartoon representation of the structure, the transmembrane domains are labelled TM1, TM2 and TM3. The conserved histidine motifs are shown in magenta (A) and the bottom view of the putative catalytic-site residues with the Histidine residues shown in stick representation and the conserved histidine motifs are labelled as 1,2, and 3 (B).

Docking studies

The membrane-bound Δ9-fatty acid desaturase uses activated oxygen molecule to create double bond between C-H bonds of saturated substrates. The enzyme particularly introduces double bond at Δ9-position of saturated palmitic and stearic acids to produce palmitoleic and oleic acids, respectively serving as the fundamental substrates for phospholipids construction and other complex lipid molecules (Castro *et al.*, 2011).

To investigate substrate specificity of *Pseudomonas* sp. A8 Δ9-fatty acid desaturase, docking studies of palmitic acid onto the modeled structure and the template were performed using Autodock software. Blind docking of palmitate and the template was first performed which showed that the palmitate was docked on the template at a site different from the vicinity of

309 the template catalytic site observed for its native ligand. Similarly, for the model structure of
310 desaturase from *Pseudomonas* A8, the docked conformation with lowest docking energy
311 formed close contact with Thr4, Trp167, Val171, Gly170, Leu175, Ala63, Cys96, Gly174,
312 Tyr95, Met141, Ile144, and Ile140 outside the catalytic site. This is expected as the COACH
313 predicted multiple binding sites on the protein.

314 It is known that the potential catalytic and binding sites for palmitate are close to the His
315 conserved motif. Therefore, specific docking was performed with grid box which covers the
316 histidine residues of the motifs. The docking simulation which produced the lowest binding
317 energy, -6.8 kcal/mol is depicted in Figure 6A. A number of residues were found in close
318 contact with the docked palmitic acid namely, Ile26, Tyr95, Val179, Gly180, Pro64, Glu203,
319 His34, His206, His71, Arg182, Thr85, Lys98 and His177 (Figure 6B). Interestingly, among
320 the binding residues are His34 and His71 and His206 from the first, second, and third
321 conserved histidine motif of the enzyme, respectively. The ligand formed two hydrogen bonds
322 with Lys98 and His177. These suggest that the docked substrate was very close to the enzyme
323 catalytic site and the conserved-histidine residues holding the metal ions of membrane-bound
324 desaturases which are known to play a key role for the enzymes catalytic activity (Shanklin *et*
325 *al.*, 2009).

326

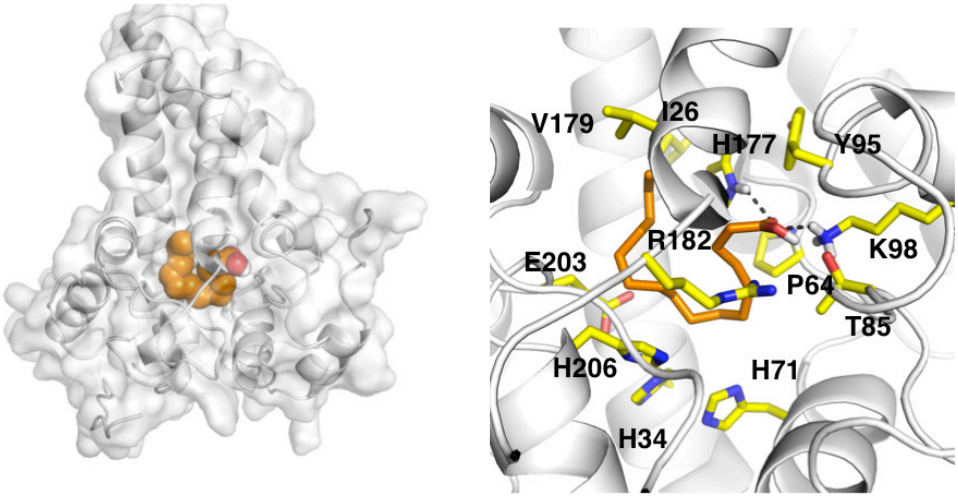

Figure 6: Docking studies of the 3D structure of palmitic acid onto the predicted model of the Δ9-fatty acid desaturase. The protein-ligand interactions are shown in surface (A) and the residues involved in binding the ligand (B) analysed using PyMOL software. Two potential hydrogen bonds predicted between Lys98 (K98) and His177 (H177) and palmitate are shown as dotted black lines.

Simulation of the predicted model of the Δ9-fatty acid desaturase in membrane

In order to further assess the Δ9-fatty acid desaturase model, the protein was embedded within a POPC bilayer and simulated for 50 ns. The approximate location of the bilayer was predicted based on the position of bilayer of the template structure. During equilibration, the protein movement was restrained for 1 ns to allow lipid molecules to equilibrate around the protein. The initial structure of the protein inside the POPC bilayer and its final structure at the end of the MD simulation are shown in Figure 7. In the membrane, the protein root mean square deviation (RMSD) was calculated to check the overall structure stability in membrane (Figure 8). The RMSD underwent major changes in the first 5 ns and become more stable after 20 ns.

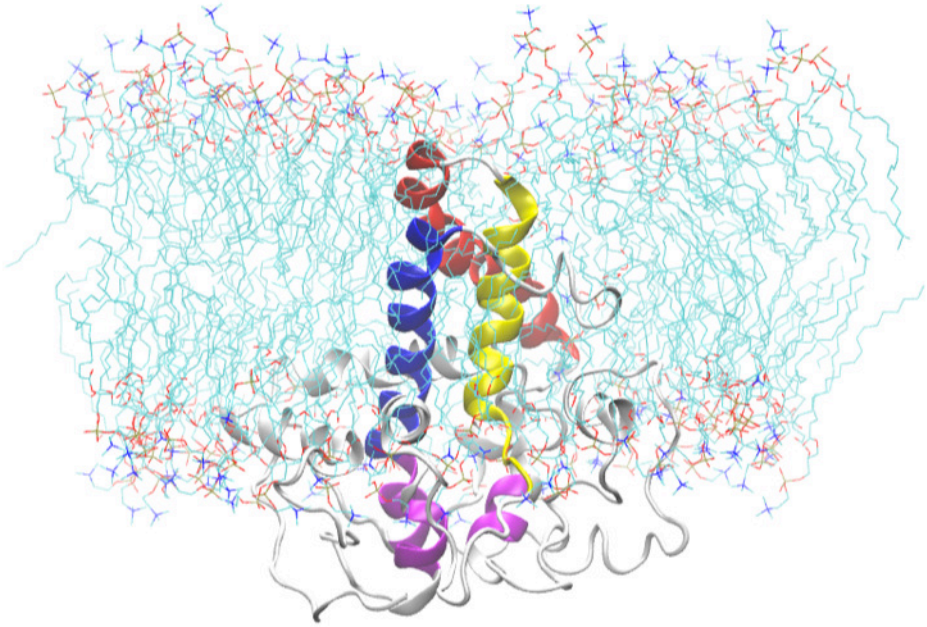

Figure 7: A snapshot of the atomistic MD simulation of the Δ9-fatty acid desaturase in POPC lipid bilayer at t=50 ns. The protein is shown in cartoon representation in grey with the TM domains coloured as blue, red, yellow for TM1, TM2 and TM3, respectively. The conserved histidine motifs are highlighted in magenta. The POPC lipid molecules are shown in line representation with carbon, nitrogen and oxygen atoms in cyan, blue and red respectively. Waters molecules are hidden for clarity.

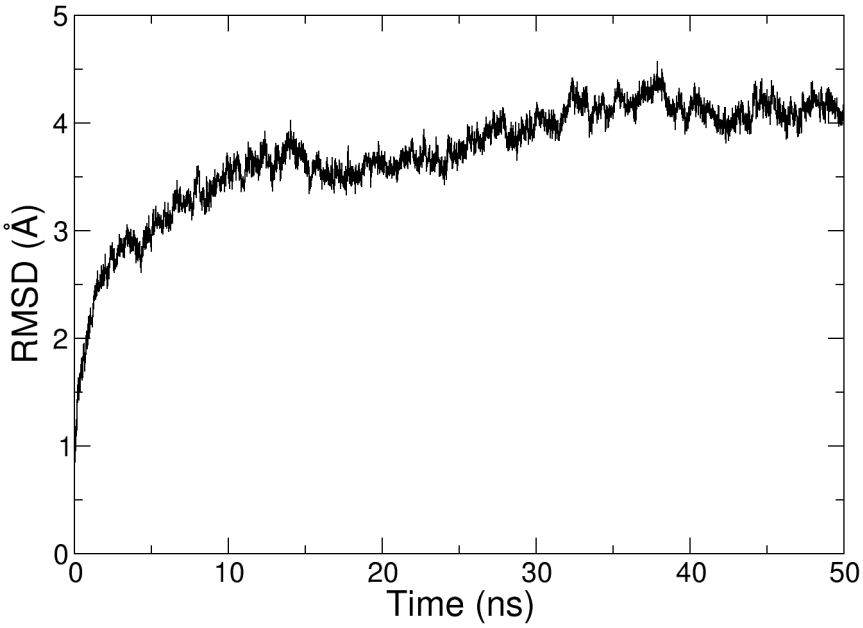

Figure 8: Total RMSD of the Δ9-fatty acid desaturase simulated in POPC lipid bilayer

Discussion

Fatty acid desaturase enzymes are involved in unsaturated fatty acid synthesis through desaturation reactions and usually have specificity for double bond insertion along the saturated acyl chains (Los and Murata, 1998; Wang *et al.*, 2013). Membrane-bound fatty acid desaturases perform dehydrogenation reactions of fatty acyl chains that are non-heme di-iron and oxygen-dependent (Meesapyodsuk *et al.*, 2007). Contrary to soluble fatty acid desaturases which have been extensively studied, structural information about the membrane-bound fatty acid desaturases is very limited. Membrane-bound fatty acid desaturases have been isolated and characterised from bacteria (Garba *et al.*, 2016a; Li *et al.*, 2008), fungi (Chen *et al.*, 2013), plants (Gao *et al.*, 2014; García-Maroto *et al.*, 2002) and animals (Bai *et al.*, 2015; Wang *et al.*, 2015). However, the only membrane-bound fatty acid desaturases that have been crystallised so far were reported from animals such as mouse stearoyl-CoA desaturase (Bai *et*

372 *al*., 2015) and human stearoyl-CoA desaturase (Wang *et al*., 2015). Both the primary
373 sequence and the modelled structure of the *Pseudomonas* sp. A8 Δ9-fatty acid desaturase
374 revealed the presence of three conserved-histidne residues at positions 34-39, 71-75 and 206-
375 210, which are typical for all membrane-bound desaturases and play a vital role for the
376 enzymes catalytic activity (Shanklin *et al.*, 2009) as shown in Figure 1 and Figure 5,
377 respectively. Moreover, multiple sequences alignments of the template and the target showed
378 an extension of amino acids (Val 253 to Ala394) at the C-terminal tail of the target which are
379 completely not observed in the template. Therefore, only residues 1 to 252 were included in
380 the model structure. However, BlastP at NCBI showed that, the extension share 93% identity
381 to both aminotransferases and acyl-CoA desaturases of many *Pseudomonas* species.

382 Contrary to the crystallised structures of other membrane-bound desaturases such as the
383 mouse stearoyl-CoA desaturase (Bai *et al*., 2015) and the human integral membrane stearoyl-
384 CoA desaturase (Wang *et al*., 2015), which both had four (4) transmembrane domains, the
385 modeled structure of the *Pseudomonas* sp. A8 Δ9-fatty acid desaturase has only three (3)
386 transmembrane domains (Figure 2) which are thought sufficient enough to span the
387 membrane bilayer twice with both protein termini facing the cytosol. Although to the best of
388 our knowledge, there was no report on the biding residues for palmitic acid from membrane-
389 bound Δ9-fatty acid desaturase, Ile26, Tyr95, Val179, Gly180, Pro64, Glu203, His34, His206,
390 His71, Arg182, Thr85, Lys98 and His177 were found to bind this substrate (Figure 6).
391 Among these residues, Ile, Val, Gly, and Arg are comparable to biding residues for stearoyl-
392 CoA by the crystallised structure of a human stearoyl-Coenzyme A desaturase (Wang *et al*.,
393 2015). Similarly, Arg, Ile, Val, Gly are comparable to some binding residues for stearoyl-CoA
394 of a mammalian steayol-CoA desaturase (Bai *et al*., 2015).

395

396 **References**

397 Alonso DL, Garcia-Maroto F, Rodriguez-Ruiz J, Garrido J, Vilches M. 2003. Evolution of
398 the membrane-bound fatty acid desaturases. *Biochemical systematics and ecology*
399 31(10):1111-1124.

400 Bai Y, McCoy JG, Levin EJ, Sobrado P, Rajashankar KR, Fox BG, Zhou M. 2015. X-ray
401 structure of a mammalian stearoyl-CoA desaturase. *Nature*.

402 Broadwater JA, Whittle E, Shanklin, J.2002. Desaturation and Hydroxylation residues 148
403 and 324 of arabidopsis fad2, in addition to substrate chain length, exert a major
404 influence in partitioning of catalytic specificity. *Journal of Biological Chemistry*
405 277(18):15613-15620.

406 Buchan DW, Minneci F, Nugent TC, Bryson K, Jones DT. 2013. Scalable web services for
407 the PSIPRED Protein Analysis Workbench. *Nucleic acids research 41*(W1), W349-
408 W357.

409 Castro LFC, Wilson JM, Gonçalves O, Galante-Oliveira S, Rocha, E., Cunha, I. 2011. The
410 evolutionary history of the stearoyl-CoA desaturase gene family in vertebrates. *BMC*
411 *evolutionary biology* 11(1):1.

412 Chen H, Gu Z, Zhang H, Wang M, Chen W, Lowther WT, Chen YQ. 2013. Expression and
413 purification of integral membrane fatty acid desaturases. *PLoS ONE* 8(3): e58139.

414 Colovos C, Yeates, TO. 1993. Verification of protein structures: patterns of nonbonded
415 atomic interactions. *Protein science* 2(9):1511-1519.

416 Dobson L, Reményi I, Tusnády GE. 2015a. CCTOP: a Consensus Constrained TOPology
417 prediction web server. *Nucleic acids research, 43*(W1), W408-W412.

418 Dobson L, Reményi I, Tusnády, GE. 2015b. The human transmembrane proteome. *Biology*
419 *direct* 10(1):31.

420 Gao L, Sun R, Liang Y, Zhang M, Zheng Y, Li D. 2014. Cloning and functional expression
421 of a cDNA encoding stearoyl-ACP Δ9-desaturase from the endosperm of coconut
422 (Cocos nucifera L.). *Gene,* 549(1):70-76.
423 Garba L, Ali MSM, Oslan SN, Rahman RNZRA. 2016a. Heterologous Expression of
424 PA8FAD9 and Functional Characterization of a Δ9-Fatty Acid Desaturase from a
425 Cold-Tolerant *Pseudomonas* sp. A8. *Molecular Biotechnology* 58(11):718-728.
426 Garba L, Ali MSM, Oslan SN, Rahman RNZRA.2016b. Molecular Cloning and Functional
427 Expression of a Δ9-Fatty Acid Desaturase from an Antarctic *Pseudomonas* sp. A3.
428 *PLoS ONE,* 11(8):e0160681.
429 García-Maroto F, Garrido-Cárdénas J, Rodríguez-Ruiz J, Vilches-Ferrón M, Adam A, Polaina
430 J, López Alonso D. 2002. Cloning and molecular characterization of the Δ6-desaturase
431 from two Echium plant species: Production of GLA by heterologous expression in
432 yeast and tobacco. *Lipids* 37(4): 417-426. Doi: 10.1007/s1145-002-0910-6
433 Hashimoto K, Yoshizawa AC, Okuda S, Kuma K, Goto S, Kanehisa M. 2008. The repertoire
434 of desaturases and elongases reveals fatty acid variations in 56 eukaryotic genomes.
435 *Journal of lipid research,* 49(1):183-191.
436 Huang J, MacKerell AD. 2013. CHARMM36 all□atom additive protein force field:
437 Validation based on comparison to NMR data. *Journal of computational chemistry*
438 34(25):2135-2145.
439 Humphrey W, Dalke A, Schulten K.1996. VMD: visual molecular dynamics. *Journal of*
440 *molecular graphics* 14(1):33-38.
441 Jo S, Kim T, Iyer VG, Im W. 2008. CHARMM□GUI: a web□based graphical user interface
442 for CHARMM. *Journal of computational chemistry,* 29(11):1859-1865.

443 Kachroo A, Shanklin J, Whittle E, Lapchyk L, Hildebrand D, Kachroo P. 2007. The
444 Arabidopsis stearoyl-acyl carrier protein-desaturase family and the contribution of leaf
445 isoforms to oleic acid synthesis. *Plant molecular biology* 63(2):257-271.
446 Laskowski RA, Moss DS, Thornton JM. 1993. Main-chain bond lengths and bond angles in
447 protein structures. *Journal of molecular biology* 23*1*(4):1049-1067.
448 Lawal G, Wahhida L, Mohd Shukuri M. 2016. Siti Nurbaya O and Raja Noor Zaliha RAR.
449 Unsaturated Fatty Acids in Antarctic Bacteria. *Research Journal of Microbiology*
450 11:146-152.
451 Lee M, Lenman M, Banaś A, Bafor M., Singh S, Schweizer M, Nilsson R, Liljenberg C,
452 Dahlqvist A, Gummeson PO. 1998. Identification of non-heme diiron proteins that
453 catalyze triple bond and epoxy group formation. *Science,* 280(5365):915-918.
454 Li Y, Dietrich M, Schmid RD, He B, Ouyang, P, Urlacher VB.2008. Identification and
455 functional expression of a Δ9-fatty acid desaturase from *Psychrobacter urativorans* in
456 *Escherichia coli*. *Lipids,* 43(3):207-213.
457 Li, Y, Xu X, Dietrich M, Urlacher VB, Schmid RD, Ouyang P, He B. 2009. Identification
458 and functional expression of a Δ9 fatty acid desaturase from the marine bacterium
459 *Pseudoalteromonas* sp. MLY15. *Journal of Molecular Catalysis B: Enzymatic*
460 56(2):96-101.
461 Lindqvist Y, Huang W, Schneider G, Shanklin J. 1996. Crystal structure of delta9 stearoyl-
462 acyl carrier protein desaturase from castor seed and its relationship to other di-iron
463 proteins. *The EMBO journal* 15(16):4081.
464 Los DA, Murata N. 1998. Structure and expression of fatty acid desaturases. *Biochimica et*
465 *Biophysica Acta (BBA)-Lipids and Lipid Metabolism,* 1394(1):3-15.

Mahgoub EO, Bolad A.2013. Correctness and accuracy of template-based modeled single chain fragment variable (scFv) protein anti-breast cancer cell line (MCF-7). *Open Journal of Genetics* 3(03):183.

Meesapyodsuk D, Reed DW, Covello PS, Qiu X. 2007. Primary structure, regioselectivity, and evolution of the membrane-bound fatty acid desaturases of *Claviceps purpurea*. *Journal of Biological Chemistry* 282(28):20191-20199.

Pronk S, Páll S, Schulz R, Larsson P, Bjelkmar P, Apostolov R, Shirts MR, Smith JC, Kasson PM, van der Spoel D. 2013. GROMACS 4.5: a high-throughput and highly parallel open source molecular simulation toolkit. *Bioinformatics,* 29(7):845-854.

Ramachandran GN, Ramakrishnan C, Sasisekharan, V.1963. Stereochemistry of polypeptide chain configurations. *Journal of molecular biology 7*(1): 95-99.

Sazinsky MH, Lippard SJ.2006. Correlating structure with function in bacterial multicomponent monooxygenases and related diiron proteins. *Accounts of chemical research 39*(8):558-566.

Shanklin J, Cahoon EB. 1998. Desaturation and related modifications of fatty acids. *Annual review of plant biology* 49(1):611-641.

Shanklin J, Guy JE, Mishra G, Lindqvist Y.2009. Desaturases: emerging models for understanding functional diversification of diiron-containing enzymes. *Journal of biological chemistry* 284(28):18559-18563.

Shanklin J, Whittle E, Fox BG. 1994. Eight histidine residues are catalytically essential in a membrane-associated iron enzyme, stearoyl-CoA desaturase, and are conserved in alkane hydroxylase and xylene monooxygenase. *Biochemistry, 33*(43), 12787-12794.

Stamm M, Staritzbichler R, Khafizov K, Forrest LR. 2013. Alignment of helical membrane protein sequences using AlignMe. *PLoS ONE 8*(3), e57731.

Trott O, Olson A J.2010. AutoDock Vina: improving the speed and accuracy of docking with a new scoring function, efficient optimization, and multithreading. *Journal of computational chemistry,* 31(2):455-461.

Venegas-Calerón M, Muro-Pastor A, Garcés R, Martínez-Force E.2006. Functional characterization of a plastidial omega-3 desaturase from sunflower (*Helianthus annuus*) in cyanobacteria. *Plant Physiology and Biochemistry,* 44(10):517-525.

Wang M, Chen H, Gu Z, Zhang H, Chen W, Chen YQ. 2013. ω3 fatty acid desaturases from microorganisms: structure, function, evolution, and biotechnological use. *Applied microbiology and biotechnology,* 97(24):10255-10262.

Webb B, Sali A. 2014. Protein structure modeling with MODELLER. *Protein Structure Prediction*, 1-15.

Yoon S, Lippard SJ. 2004. Water-dependent reactions of diiron (II) carboxylate complexes. *Journal of the American Chemical Society* 126(51):16692-16693.